

# Design Optimization of Micro Air Launch Vehicle Using Differential Evolution

Mohammed Abdulmalek Aldheeb<sup>1,\*</sup>, Raed Kafafy<sup>1</sup>, Moumen Idres<sup>1</sup>, Hanafy M. Omar<sup>2</sup>, Mohammad A. Abido<sup>3</sup>

<sup>1</sup>International Islamic University Malaysia - Kuala Lumpur – Malaysia

<sup>2</sup>Qassim University - Buraidah – Saudi Arabia

<sup>3</sup>King Fahd University of Petroleum and Minerals - Dharhan – Saudi Arabia

**Abstract:** In this paper, we have used the differential evolution to optimize the design of a Micro Air Launch Vehicle and its launch trajectory. Since trajectory design of a launch vehicle requires prior knowledge of the masses and propulsion performance parameters of the Micro Air Launch Vehicle, whereas the vehicle design requires prior knowledge of the required velocity ( $\Delta V$ ) to insert the required payload into the target orbit, a two-step optimization cycle was adopted. A Micro Air Launch Vehicle was designed to launch a 20-kg payload into a 400-km circular polar orbit. The preliminary design of the Micro Air Launch Vehicle was conducted given the required  $\Delta V$ , which was obtained from trajectory optimization, and then applied in mission analysis to obtain the initial masses. These initial masses were used in the vehicle design to get the performance and geometry parameters. The objective function of the Micro Air Launch Vehicle design optimization is to minimize the initial mass under specified constraints on the insertion orbit. The objective of trajectory optimization is to maximize the payload mass under constraints on orbit specifications and design variables. For the 20-kg payload mass, the optimal initial mass is 1267.8 kg and optimal payload is 20.6 kg, which slightly exceeds the mission requirements.

**Keywords:** Micro Air Launch, Vehicle design, Optimization, Differential evolution.

## LIST OF SYMBOLS

$A_e$ : Exit area  
 $A_t$ : Throat area  
 $A_w$ : Wall area (surface area)  
 $c$ : Effective exhaust velocity  
 $CF$ : Thrust coefficient  
 $D$ : Rocket diameter  
 $\varepsilon$ : Expansion ratio  
 $F$ : Thrust  
 $f$ : Velocity fraction of each stage  
 $f_{inert}$ : Inert mass fraction  
 $I_{sp}$ : Specific impulse  
 $L$ : Rocket length  
 $L/D$ : Length to diameter ratio  
 $m_{cs}$ : Motor case mass  
 $M_e$ : Exit Mach number

$m_i$ : Initial mass  
 $m_{inert}$ : Inert mass  
 $m_{insul}$ : Insulation mass  
 $m_{pay}$ : Payload mass  
 $m_{prop}$ : Propellant mass  
 $m_{pv}$ : Pressure vessel mass  
 $m_{sk}$ : Skirt mass  
 $\dot{m}$ : Mass flow rate  
 $NDF$ : Nozzle diameter fraction ( $D_{nozzle}/D_{motor}$ )  
 $Pa$ : Ambient pressure  
 $P_c$ : Chamber pressure  
 $P_e$ : Exit Pressure  
 $t_b$ : Burning time  
 $T/W$ : Thrust to weight ratio  
 $v$ : Velocity  
 $V_{cs}$ : Motor case volume  
 $\gamma$ : Specific heat  
 $\varepsilon$ : Expansion ratio  
 $\theta_{cn}$ : Half cone nozzle angle  
 $\rho$ : Density  
 $\alpha$ : Angle of attack

Received: 15/01/12

Accepted: 16/03/12

\*author for correspondence: aldheeb750@yahoo.com

P.O. Box 10, 50728 Kuala Lumpur/Malaysia

## INTRODUCTION

Air launch has received increasing attention over the last decades, due to the many advantages it has over ground launch. An air-launch vehicle is released from a flying carrier (aircraft), which significantly alleviates many launch restrictions and virtually allows launching at any desired location and in any launch azimuth. Air launch takes advantages of the carrier altitude and velocity that improves the launch efficiency and reduces the initial mass of the launch vehicle. With the advance of Microelectronics and Micro-Electro-Mechanical Systems (MEMS), it became possible for micro- (less than 100 kg) or nano-satellites (less than 10 or 20 kg) to perform the typical functions of larger satellites in the last decade (Fortescue *et al.*, 2003, Matsuda *et al.*, 2008).

To reduce launching costs, such small satellites are usually launched from the ground with many other small satellites or as a secondary payload to a main larger one. Thus, the small satellite mission becomes constrained by the mission requirements of the main payload. Using air launch, small satellites can be independently launched and be not constrained by the mission specifications of another payload. Responsivity is another main advantage of the air launch, especially during time of crisis because its preparation is much less time-demanding than ground launch (Boltz, 2002). In order to take full advantage of air launch, its vehicle should be designed with the right size for the payload. Nowadays, operational air launch vehicles, such as Pegasus series (Braun *et al.*, 1997, Isakowitz *et al.*, 2004), are designed for payloads that are far above nano-satellites making them inefficient for launching a single or a few nano-satellites. The design of very small air launch vehicles was investigated by Boltz (2001), Choi *et al.* (2009) and Omar *et al.* (2011). Miniaturization of air launch vehicles is seen in a major problem, which is the increase of inert mass fraction or the decrease of vehicle mass ratio (payload mass to total mass ratio) as the payload mass is decreased.

Earlier research in rocket design used several optimization techniques. Lee *et al.* (2002; 2007) studied the trajectory optimization of air-launch rocket using the Multidisciplinary Design Optimization (MDO) technique. In their method, rocket sizing, trajectory and propulsion analyses are coupled altogether. In the two-step method, mission requirements are optimized in one and then the trajectory and propulsion analyses are optimized in the second step. The optimization used is called multidisciplinary feasible optimization. Choi *et al.* (2009) used sequential quadratic programming (SQP).

In this paper, we have optimized the design of a micro air launch vehicle (MALV) to achieve minimum initial mass. The optimization of the MALV is carried out in two steps; the first is to optimize the vehicle for minimum initial mass and the second is to optimize the trajectory for maximum payload mass. Due to the complexity of the optimization problem, we use differential evolution (DE). It is a population stochastic optimization technique that belongs to the class of evolutionary algorithms, it is also a promising optimization for single- and multi-objective optimization and it has a good convergence properties. The main advantages of DE are its simplicity, accuracy, and reasonably fast and robust optimization method (Wong and Dong, 2005).

To initiate the two-step optimization cycle, we use a set of scaling laws to estimate the initial guess of the masses and performance parameters of MALV, which is capable of launching the required payload into the target orbit. The cubic scaling law is used to downsize the rocket mass to miniaturize the rocket for small payloads and to study an alternative low-cost system in Responsive Access Small Cargo Affordable Launch (RASCAL) (Sutton and Biblarz, 2010; Humble *et al.*, 1995). Boltz (2002) has shown that the actual payload mass of a miniaturized air launch vehicle will be much smaller than predicted by cubic laws, due to the non-scalability of avionics and navigation and guidance systems. However, Omar *et al.* (2011) have shown that the great reduction of the mass and size of electronic devices, due to advancements in microelectronics, makes it possible to assume cubic law scaling with some conservation.

## DIFFERENTIAL EVOLUTION ALGORITHM

DE was first proposed by Storn and Price (1997) at Berkeley as a new evolutionary algorithm. It uses a function called crossover to increase the diversity of the perturbed parameter vectors, and it ensures that the last vector gets at least one parameter from the previous one (Storn and Price, 1997; Storn, 1996). As a population-based algorithm, the DE starts with a set of candidate solutions. The initial solutions are randomly generated over the problem space. The steps of DE algorithm can be described as follows (Storn and Price, 1995; 1996; 1997; Abou El Ela *et al.*, 2011; Abido and Al-Ali, 2009):

- Initialize stochastic solutions as in Eq. 1:

$$x_{ij} = x_{j\text{-lower limit}} + r(x_{j\text{-upper limit}} - x_{j\text{-lower limit}}) \quad (1)$$

where,  $r$  is a random number,  $r \in [0,1]$ .

- Evaluate each initial solution against the objective function.
- Check the stopping criteria. Stop, if they are satisfied.
- For each solution  $x_p$ , create a mutant solution  $x'_i$  as follows by randomly selecting three different solutions (R1, R2, R3), as in Eq. 2.

$$x'_i = x_{R1} + F(x_{R3} - x_{R2}) \quad (2)$$

where,  $F$  is a mutation factor between  $[0,1]$ .

- For each mutant solution, generate a trial solution  $x''_i$  by copying parameters either from the parent solution  $x_i$  or the mutant one  $x'_i$  as Eq. 3

$$x''_{i,j} = \begin{cases} x'_{i,j} & \text{if } \text{rand}(0,1) < CR \\ x_{i,j} & \text{else} \end{cases} \quad (3)$$

where,  $CR$  is a specified crossover factor between  $[1, 0]$  and the subscript  $j$  refers to the  $j$ th dimension of the solution vector.

- Evaluate each trial solution against the objective function.
- Compare the objective function of the trial solution with that of the parent solution. Select the better solution to survive in the next generation.
- Repeat steps four to seven until the population is filled.
- Update the best solution and go to step three.

In this paper, we have taken the mutation constant ( $F=0.9$ ), the crossover constant ( $CR=0.7$ ), the size of population ( $NP=40$ ). The search will be terminated if the number of iterations, since the last change of the best solution is greater than 50, or such number reaches 150 and 500 for design and trajectory optimizations, respectively.

### DESIGN PROCESS

The whole design process is illustrated in a flowchart shown in Fig. 1. The design flow chart is further elaborated.

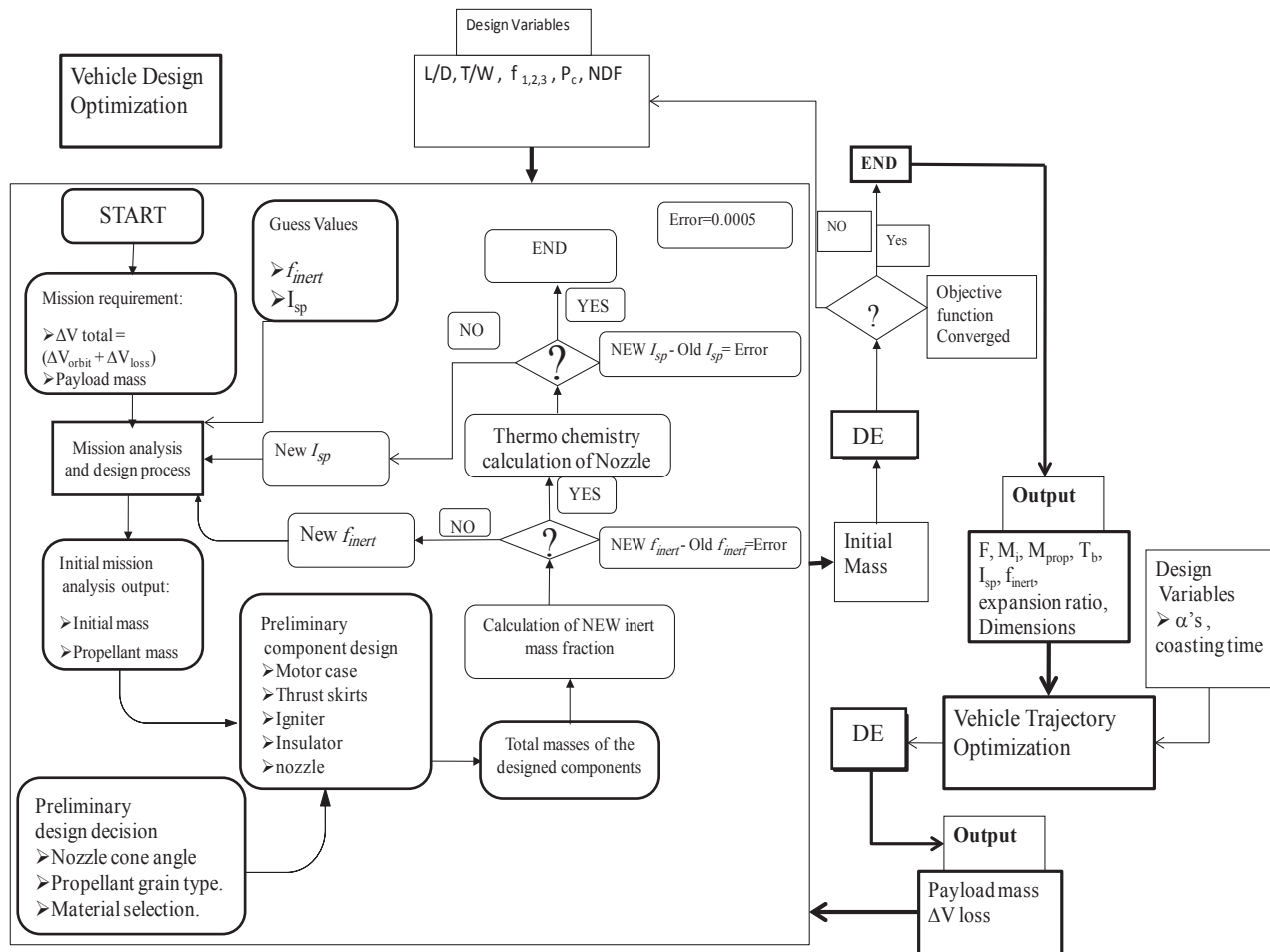


Figure 1. Chart of vehicle design and trajectory optimization of air-launch vehicle using differential evolution

## Design requirements

### Mission requirements

Mission requirements are the target parameters to be achieved in the design process. Some requirements may be considered as constraints on the design, which are:

### Orbit and altitude

MALV should be able to insert its payload into a 400-km circular polar orbit.

### Payload mass

MALV should be able to launch at least 20 kg into the target orbit.

### Launch conditions

MALV will be launched from a carrier aircraft at an altitude of 12 km and speed of 300 m/s.

### Decisions

Certain parameters should be defined to start the design process. They are selected based on published data of existing launch vehicles (e.g. Pegasus). However, some of them will be set as design variables in the optimization stage in order to find the optimal values. These parameters are: the number of stages (we have decided to use three, fixed); the type of rocket in each stage (we choose solid motor rocket with end burning grain propellant, fixed); chamber pressure ( $P_c$ ); thrust-to-weight ratio ( $T/W$ ); length to diameter ratio ( $L/D$ );  $T/W$  and  $L/D$  will be set as design variables in the optimization process.

### Initial values

To start the design process, initial values for specific impulse ( $I_{sp}$ ) and inert mass fraction ( $f_{inert}$ ) are required. However, these values will change during the design loop processes until their values are converged. An initial value of total  $\Delta V$  is also required to start the design process.

## Design of micro air launch vehicle subcomponents

The required  $\Delta V$  is used in mission analysis with initial specific impulse and inert mass fraction. The output of mission analysis is the initial values of propellant and inert masses using Eq. 4 and Eq. 5

$$m_{prop} = \frac{m_{pay} \left( \frac{\Delta V}{e^{I_{sp} g_0} - 1} \right) (1 - f_{inert})}{1 - f_{inert} e^{\frac{\Delta V}{I_{sp} g_0}}} \quad (4)$$

$$m_i = m_{prop} + m_{payload} + m_{inert} \quad (5)$$

Note that the selected  $\Delta V$  at the first step of the design is taken based on some previous available data of Pegasus to start the design process. However, this  $\Delta V$  will be replaced by the real value when the trajectory analysis is performed.

The propellant masses along with  $T/W$ ,  $L/D$ , and chamber pressure are used to design the geometry of the vehicle and to obtain the initial masses again and also to obtain the inert mass fraction. The vacuum thrust of the vehicle can be calculated using Eq. 6:

$$F = \dot{m} v + A_e P_e \quad (6)$$

Figure 2 illustrates the main components of MALV. Solid motor has a classical architecture and is attached to the other stages by thrust skirts. The volume is calculated using the propellant mass and its density, a cylindrical motor case with half dome ends is selected for the design as shown in Fig. 3, the calculations are done using Eqs. 7 to 12:

$$V_{cs} = \frac{m_{prop}}{n_{sp} \rho_{prop}} \quad (7)$$

$$V_{cs} = \pi D^3 \left[ \frac{1}{6} + \frac{1}{4} \left( \frac{L}{D} - 1 \right) \right] \quad (8)$$

Pressure vessel and skirt masses are calculated using Eqs. 9 to 12 (Humble, 1995):

$$m_{pv} = \rho_{cs} t_{cs} D^2 \pi \left( 1 + \frac{L_{cy}}{D} \right) b \quad (9)$$

$$m_{sk} = \rho_{cs} t_{cs} \pi D^2 \quad (10)$$

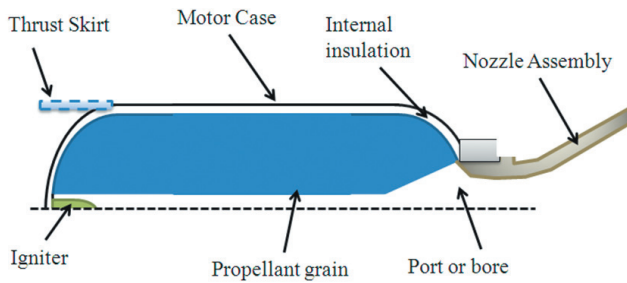


Figure 2. Main components of the solid rocket motor.

Thus, the motor case mass is:

$$m_{cs} = 1.1(m_{sk} + m_{pv}) \quad (11)$$

Insulation mass of motor case is

$$m_{insul} = 1.788 \times 10^{-9} m_{prop}^{-1.33} t_b^{0.965} \left(\frac{L}{D}\right)^{-0.144} L_{sub}^{0.058} A_w^{2.69} \quad (12)$$

The nozzle parameters are shown in Fig. 4 and calculated using Eqs. 13 to 20. Nozzle system mass may be calculated from Eq. 13 (Humble, 1995).

$$m_{noz\_sys} = 1.5 \left\{ 0.256 \times 10^{-4} \left[ \frac{(m_{prop} c^*)^{1.2} \varepsilon^{0.3}}{P_c^{0.8} t_b^{0.6} \tan \theta_{cn}} \right] \right\} \quad (13)$$

The throat diameter and nozzle length are calculated using Eqs. 14 and 15:

$$D_t = \sqrt{\frac{4c^* m_{prop}}{\pi t_b P_c}} \quad (14)$$

$$L_{noz} = \frac{D_e - D_t}{2 \tan \theta_{cn}} \quad (15)$$

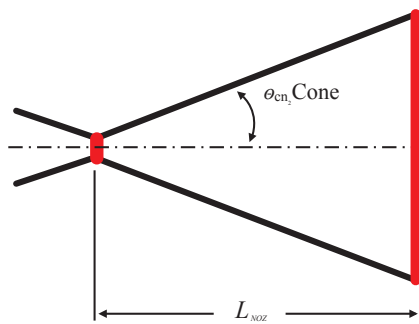


Figure 4. Sketch of nozzle design.

In this work, the inert mass of each stage was calculated from the sum of the motor case, the insulation, and the nozzle system masses. The inert mass includes also avionics, separation systems, attitude control systems, and so on. This may

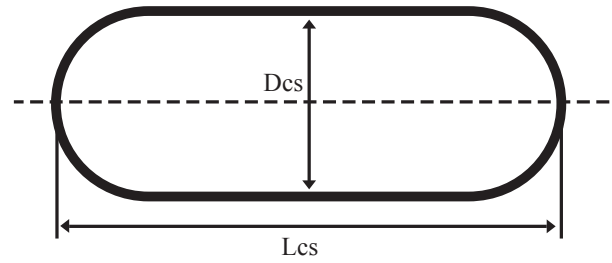


Figure 3. Sketch, length, and diameter of the motor case.

comprise an important fraction of the payload mass, especially in the upper stages, which become more profound in the case of small payloads. Thus,

$$m_{inert} = m_{cs} + m_{insul} + m_{noz\_sys} \quad (16)$$

The inert mass fraction is calculated again using the new inert mass as in Eq. 17:

$$f_{inert} = \frac{m_{inert}}{m_{inert} + m_{prop} - m_{pay}} \quad (17)$$

If this new inert mass fraction is not the same as the initial values, then the new finert will be used in mission analysis and the same steps will be repeated until finert converges. When finert is converged, then the value of Isp should be evaluated and compared with initial values, if it is not the same, the whole previous procedure will be repeated until the solution of Isp and finert converges. The calculation of the nozzle specific impulse is done using Eqs. 18 and 19 (Sutton and Biblarz, 2010):

$$\varepsilon = \frac{1}{M_e} \sqrt{\left[ \left( \frac{2}{y+1} \right) \left( 1 + \frac{y-1}{2} M_e^2 \right) \right]^{\frac{y+1}{y-1}}} \quad (18)$$

$$P_e = P_c \left[ 1 + \frac{y-1}{2} M_e^2 \right]^{\frac{y}{y-1}} \quad (19)$$

$$C_F = \sqrt{\left( \frac{2y^2}{y-1} \right) \left( \frac{2}{y+1} \right)^{\frac{y+1}{y-1}} \left[ 1 - \left( \frac{P_e}{P_c} \right)^{\frac{y-1}{y}} \right]} + \frac{\varepsilon(P_e - P_a)}{P_c} \quad (20)$$

$$I_{sp} = \frac{\lambda C_F c^*}{g_0} \quad (21)$$

Output of the vehicle design is total mass, propellant mass, inert mass, specific impulse, inert mass fraction, dimensions, nozzle expansion ratio, thrust, mass flow rate, and burning time.

In the case of a vehicle requiring real developments, the targeted payload mass should have a margin to cover

inevitable losses during the development, which may cause a substantial loss in the targeted final mass.

### Trajectory analysis

Since the  $\Delta V$  loss was selected based on published data of existing launch vehicles, a trajectory analysis was needed to obtain a more realistic  $\Delta V$  loss of the MALV.

### Aerodynamic model

Missile Datcom is the software used to obtain aerodynamic coefficients of lift and drag using the dimensions obtained from the design of MALV subcomponent. These coefficients are obtained for the first stages, assuming that at the second one the effects of aerodynamic forces are negligible. Fig. 5 shows the acting forces of MALV body in 2D.

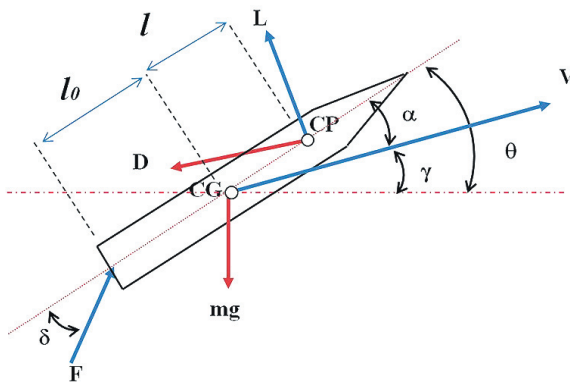


Figure 5. Two dimensional body forces for flying vehicle.

Since the aerodynamic forces coefficients are obtained, the trajectory model is done using the equations of motion numbers 22 and 23 (Fortescue, *et al.*, 2003):

$$m \frac{dV}{dt} = F \cos(\delta + \alpha) - mg \sin \gamma - D \quad (22)$$

$$mv \frac{dv}{dt} = L + F \sin(\delta + \alpha) - mg \cos \gamma + \frac{mV^2}{r} \cos \gamma \quad (23)$$

The total  $\Delta V$ , which is required from the launch vehicle, is calculated from Eq. 24:

$$\Delta V_{total} = V_{orbit} - V_{aircraft} + \Delta V_{loss} \quad (24)$$

where,  $\Delta V_{loss}$  is the summation of drag, gravity, steering, and performance losses, which can be expressed as Eq. 25:

$$\Delta V_{loss} = \Delta V_{drag} + \Delta V_{gravity} + \Delta V_{steering} + \Delta V_{performance} \quad (25)$$

In the Eq. 25,  $\Delta V_{gravity}$  is the velocity needed to overcome the effect of the gravity and gain altitude and  $\Delta V_{drag}$  is the loss due to drag that is profound at low altitudes, but become negligible at high ones.  $\Delta V_{steering}$  is the velocity needed to steer and turn the vehicle along the trajectory.  $\Delta V_{performance}$  is the velocity loss due to ideal performance assumptions, since vacuum performance is assumed during the design, whereas the actual rocket performance is reduced by atmospheric pressure.

### STEP 1: MICRO AIR LAUNCH VEHICLE DESIGN OPTIMIZATION

The optimization of MALV aims at finding the best values of design variables in order to minimize the initial mass of the vehicle. The optimization of the MALV algorithm is the almost the same as its design procedure; the difference is the range of design variables. Four parameters were selected as the design variables at each stage:  $T/W$ ,  $L/D$ ,  $D_{nozzle}/D_{motor}$  and  $f$ . The total number of design variables is 15. Each one has a reasonable range, so they are not over or under estimated. The range values of these design variables are listed in details for stages 1 to 3 in the following section of optimization constraints.

#### Optimization constraints

In the optimization, the number of generations was taken as 150 with a number of particles of 15. The mission defined is to launch a 20 kg payload to a 400 km circular polar orbit from an altitude of 12 km with initial velocity of 300 m/s. The initial velocity loss was guessed at 2,000 m/s; which was considered pessimistic after the first two-step optimization cycle. A more realistic value of 1,500 m/s was used in the final two-step optimization cycle, a fact that is compared fairly well to the value calculated by trajectory simulation for the optimized vehicle and trajectory. The range of design variables for each stage is further given.

#### Stage 1

$$\begin{aligned} 3 &\leq T/W \leq 3.5 \\ 7.5 &\leq L/D \leq 9 \\ 0.8 &\leq NDF \leq 1 \\ 0.3 &\leq f_1 \leq 0.5 \end{aligned}$$

**Stage 2**

$$3 \leq T/W \leq 3.5$$

$$2.5 \leq L/D \leq 5$$

$$0.5 \leq NDF \leq 0.68$$

$$0.25 \leq f_2 \leq 0.5$$

**Stage 3**

$$3 \leq T/W \leq 4$$

$$1.7 \leq L/D \leq 4$$

$$0.4 \leq NDF \leq 0.6$$

$$f_3 = 1 - f_1 - f_2$$

**Micro air launch vehicle design optimization results**

**Optimal design variables**

The design variables shown in Fig. 6 to 9 represent the optimal values that provide the optimal initial mass of MALV. High  $D_{nozzle}/D_{motor}$  provides better results, since it increases the expansion ratio and results in better performance and less initial mass. The minimum initial mass (objective function) obtained is 1,287.3 kg for payload of 20 kg to 400-km circular polar orbit. The objective function evolution along the optimization is shown in Fig. 10, and the optimal values of the design variables are shown in Table 1.

Table 1. Optimal design variables of MALV.

Design variable	Stage 1	Stage 2	Stage 3
$M_i$ (kg)	1287.34	385.8757	105.408
$T/W$	3	3	4
$L/D$	7.5	2.5	1.7
$D_{nozzle}/D_{motor}$	1	0.68	0.6
$f$	0.3	0.3041	0.3959

Table 2 shows the design parameters obtained at the optimal design variables. It represents the output of the design optimization process for the mass, geometry, and performance parameters of MALV. The thrust, masses, and dimensions are high in the first stage and low in the third stage, but the values of burning time, expansion ratio, specific impulse, mass fraction, and velocity fraction are not. The expansion ratio has a high value in the third stage and low in the first one.

Table 2. Optimal MALV parameters.

Parameter	Stage 1	Stage 2	Stage 3
Thrust (N)	37311.85	11050.59	3873.561
Length (m)	4.080286	1.629353	0.938153
Inert mass (kg)	113.7089	39.49656	10.56858
Throat area (m <sup>2</sup> )	0.002691	0.000839	0.000272
Exit area (m <sup>2</sup> )	0.157146	0.073051	0.03366
Expansion ratio	58.40634	87.09153	123.8406
Burning time (s)	58.30218	61.06214	50.51115
Diameter (m)	0.447309	0.448496	0.345035
Initial mass (kg)	1267.817	375.4873	98.71461
Propellant mass (kg)	778.6207	237.2761	68.14603
Inert mass fraction	0.127429	0.142704	0.134265
Thrust fraction	1.849018	1.882084	1.900171
Specific impulse (s)	284.7978	289.8908	292.6767
Velocity fraction	0.3	0.320485	0.379515

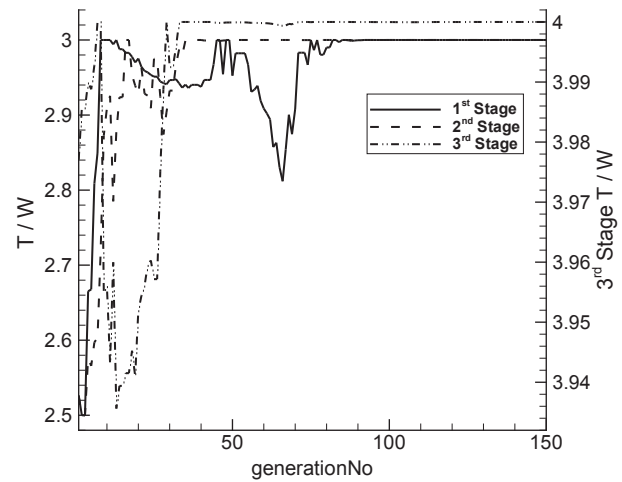


Figure 6. Thrust-to-weight optimal values.

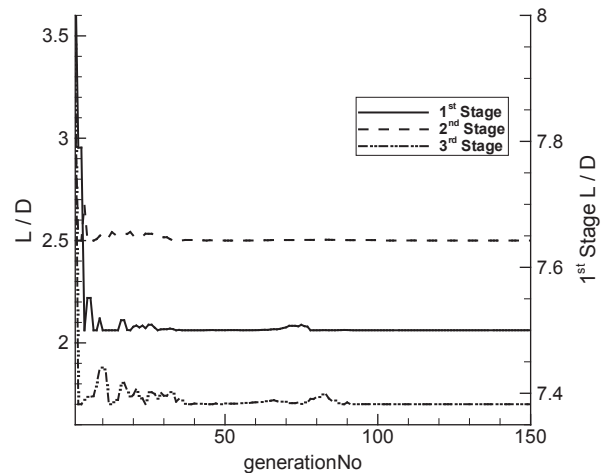


Figure 7. Length-to-diameter optimal values.

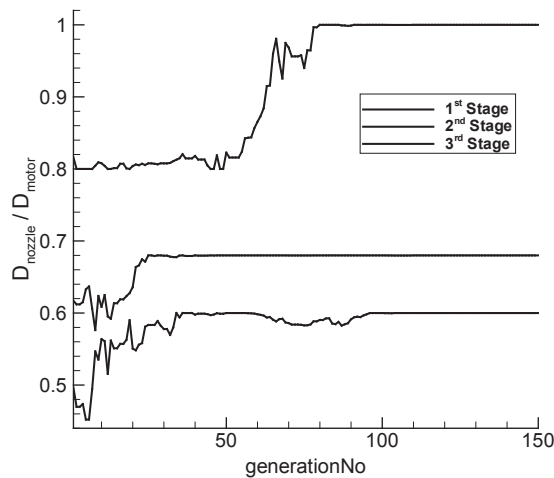


Figure 8. Optimal value of exit nozzle diameter to motor case diameter ratio.

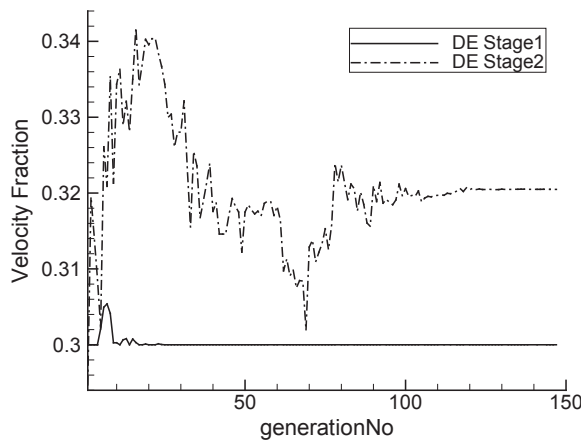


Figure 9. Velocity fraction evolution.

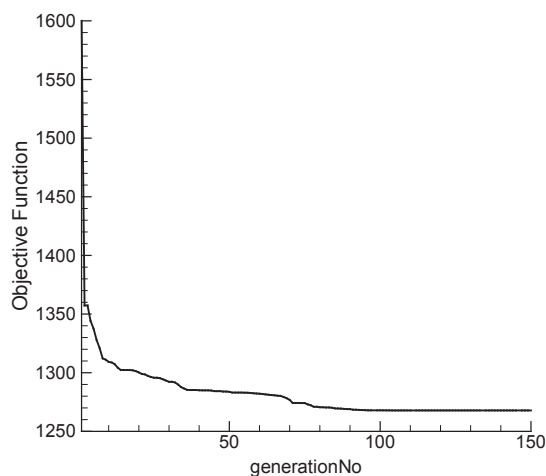


Figure 10. Optimal objective function of vehicle design.

The exit diameter of the nozzle is fixed by a certain range of values related to the diameter of motor case, which

is controlled by L/D ratio. The throat diameter is obtained using Eq. 26,

$$D_t = \sqrt{\frac{4c^* m_{prop}}{\pi t_b P_c}} \quad (26)$$

The values of  $c^*$  and  $P_c$  are the same for all stages and there is not a very much difference in burning time. Thus, propellant mass is the parameter that significantly affects the throat area and we can see from Table 2 that the propellant mass is very small for the third stage compared to the first, resulting in a small value of the throat area. Therefore, the expansion is high for the third stage and high expansion ratio is good and required at high altitude.

## Step 2: Trajectory Optimization

In this step, the trajectory is optimized to get the maximum payload mass. The trajectory model is done using equations of motion (Eqs. 22 and 23).

The inputs of trajectory optimization are: initial mass, propellant mass, burning time, specific impulse, and thrust (Table 3). Trajectory optimization has three important factors: the objective function, the design variables, and the constraints. The objective function is the payload mass, the design variables are angles of attack ( $\alpha$ ), third stage coasting time, and payload mass. The payload mass and the design variables are the objective functions, since payload is used in the calculations. The constraints are very important to achieve the desired orbit and velocity, and they are called penalty function. This penalty function calculates the error in altitude, insertion velocity and flight path angle between the real and calculated values from the trajectory optimization. Thus, the optimization should achieve the optimal objective function and should also match the constraints. The design variables of the trajectory optimization are shown in Table 4. The number of generations was taken as 500 with 40 individuals in each generation.

Table 3. Input parameters for trajectory optimization.

	Stage 1	Stage 2	Stage 3
$F$ (N)	37311.85	11050.59	3873.561
$A_e$ (m <sup>2</sup> )	0.157146	0.073051	0.03366
$t_b$ (s)	58.30218	61.06214	50.51115
$m_i$ (kg)	1267.817	375.4873	98.71461
$m_{prop}$ (kg)	778.6207	237.2761	68.14603
$I_{sp}$ (s)	284.7978	289.8908	292.6767

The convergence of the objective function of trajectory optimization is shown in Figs. 11 and 12. Table 5 shows the

Table 4. Design variable range of trajectory optimization.

Design variables	Range
$\alpha_1$ (deg)	1-4
$\alpha_2$ (deg)	2-5
$\alpha_3$ (deg)	3-6
$\alpha_4$ (deg)	3-7
$\alpha_5$ (deg)	5-9
$\alpha_6$ (deg)	0-3
$\alpha_7$ (deg)	0-3
$\alpha_8$ (deg)	0-3
$\alpha_9$ (deg)	0-3
$\alpha_{10}$ (deg)	0-5
Coasting time (s)	260-390
Payload mass (kg)	19-23

best values of design variable of  $\alpha$  and third stage coasting time, which provide the best trajectory shown in Fig. 13. This trajectory is the optimal one that maximum payload can be carried through to the required altitude. The payload obtained from trajectory optimization is 20.6 kg, while it is 20 kg in MALV design.

The performance of  $\alpha$ 's through the optimization process is shown in Figs. 14 and 15. The evolution of the 3rd stage burning time is shown in Fig 16. Figure 17 shows the increasing in the payload mass along the optimization; the payload mass increases until it reach steady state which is the optimal value of the payload mass.

The effect of angles of attack is mainly at the first stage, where effect of lift and dynamic pressure are high. The time

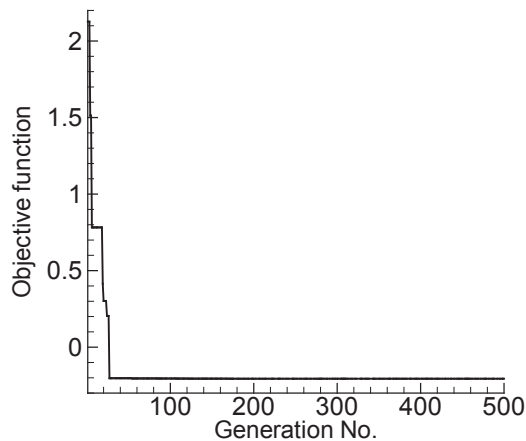


Figure 11. Objective function evolution of trajectory.

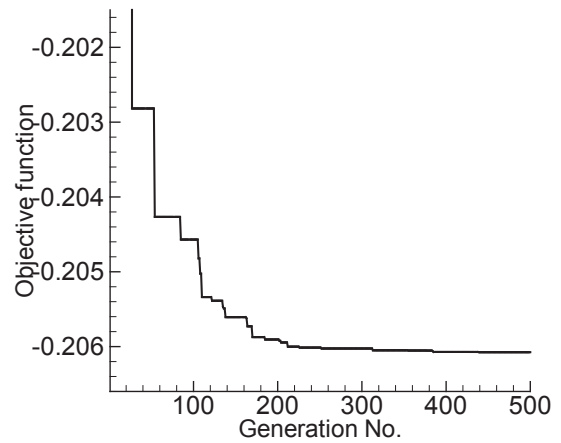


Figure 12. Zoomed objective function to show the convergence.

Table 5. Optimal values of design variables.

Design variable	Optimal values	Time of $\alpha$ change
$\alpha_1$ (deg)	1.827477	0
$\alpha_2$	4.714505	5
$\alpha_3$	5.525553	7.9151
$\alpha_4$	6.170552	10.8302
$\alpha_5$	8.628338	19.5755
$\alpha_6$	1.786781	31.6511
$\alpha_7$	2.866733	66.8022
$\alpha_8$	1.414886	127.8407
$\alpha_9$	0.772816	414.1451
$\alpha_{10}$	1.936009	464.6709
3 <sup>rd</sup> stage coasting time (s)	286.3128	
payload mass (kg)	20.6074	
$\Delta V_{loss}$ (m/s)	1382.75	

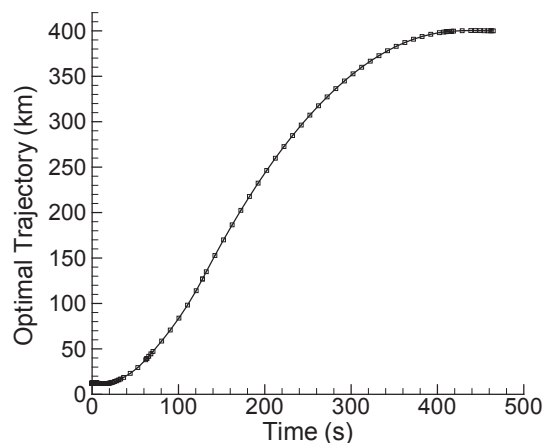


Figure 13. Optimal trajectory.

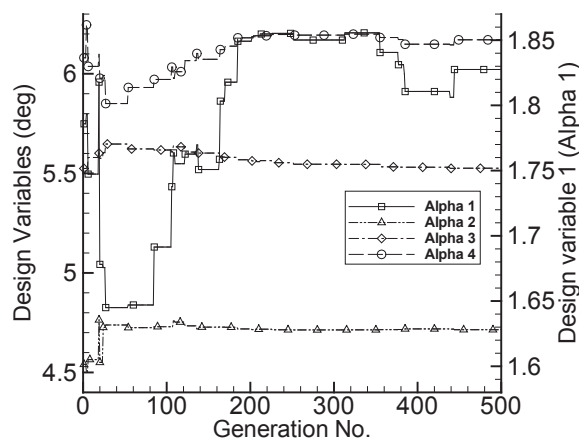


Figure 14. Design variables alpha 1 to 4.

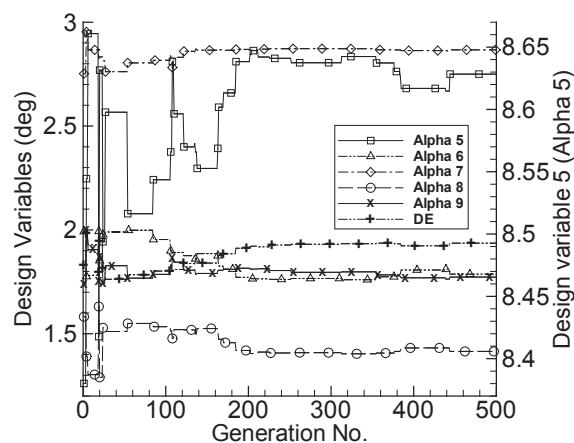


Figure 15. Design variables alpha 5 to 10.

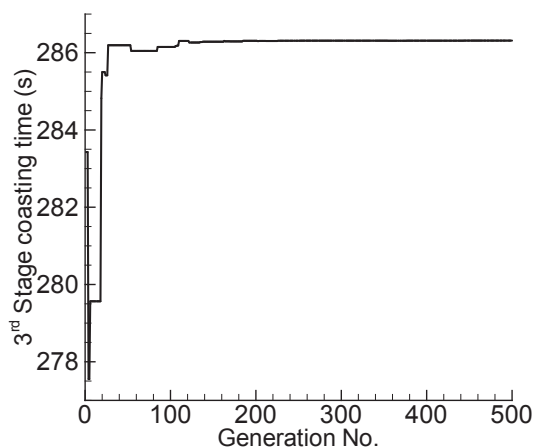


Figure 16. Design variable, third stage coasting time.

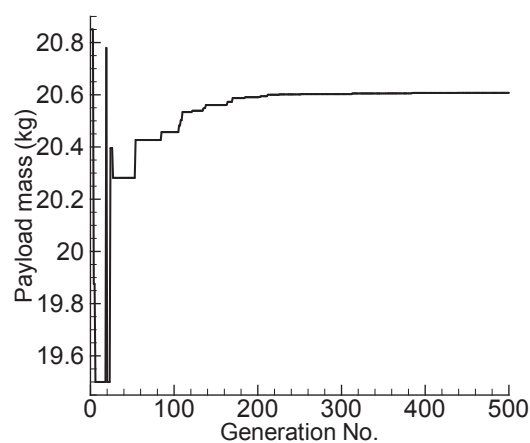


Figure 17. Payload mass evolution.

of changing alpha is shown in Table 5, in which there are six values of  $\alpha$  used in the first stage. Figure 18 shows the optimal value of angle of attack along the trajectory from the ignition point until the insertion one in the orbit.

The  $\Delta V_{loss}$  due to steering, gravity and drag is shown in Fig. 19. The value of total  $\Delta V_{loss}$  obtained from the trajectory is 1,382 m/s, while the one used in  $\Delta V_{loss}$  in the design optimization is 1,500 m/s. The difference  $\Delta V_{loss}$  is about 110 m/s and it is called  $\Delta V_{performance}$ , this value is a correction of the performance because in design we assumed a vacuum thrust, but the first stage does not perform in a vacuum. Thus, this  $\Delta V_{loss}$  is the correction value of the vehicle performance.

## SUMMARY AND CONCLUSIONS

In this paper, we have developed a two-step DE optimization algorithm for the design optimization of MALV. In the first step, the vehicle design parameters were optimized for minimum initial mass, given the total trajectory

velocity loss. In the second step, the vehicle trajectory was optimized for maximum payload, and total velocity loss was calculated. The two-step optimization cycle is repeated until there is an acceptable convergence of the total velocity loss. Only a few two-step optimization cycles are needed to reach a reasonably convergent value of total velocity loss, which was taken as 1,380 m/s.

The optimization process was repeated several times with different starts to assure that the obtained optimal design is as close as possible to the actual optimal design. The optimization was started from three to five times for 200-400 iterations in each start, without changing input parameters to ensure that the optimization achieves a reliable optimal solution.

In vehicle design optimization, we have concluded that higher nozzle diameter fraction values provide better performance and less initial mass of MALV. T/W and L/D affect other parameters, such as thrust, expansion ratio, and specific impulse. For the selected mission requirement, the initial mass obtained in MALV design optimization is 1,267.8 kg for a 20-kg payload mass.

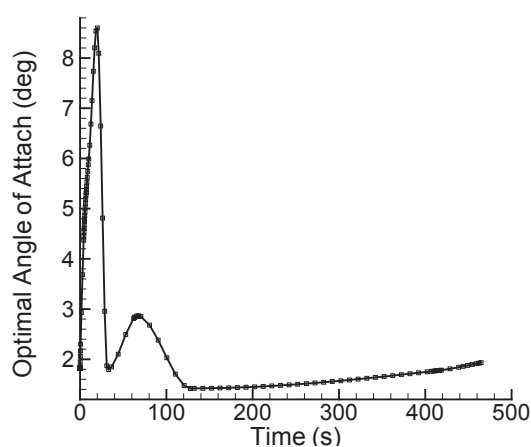


Figure 18. Optimal angle of attack along the trajectory.

In trajectory optimization, ten angles of attack were used as design variables. The optimal payload that can be launched into 400-km polar circular orbit is 20.6 kg, with a small increase in payload mass over the target payload mass.

#### ACKNOWLEDGMENTS

This work was partially supported by endowment research fund from the International Islamic University of Malaysia.

#### REFERENCES

- Abou EL Ela, A. A. *et al.*, 2011, "Differential Evolution Algorithm for Optimal Reactive Power Dispatch", *Electric Power Systems Research*, Vol. 81, No. 2, pp. 458-464.
- Abido, M. A. and Al-Ali, N. A., 2009, "Multi-objective differential evolution for optimal power flow", *International Conference on Power Engineering, Energy and Electrical Drives*, 2009. POWERENG09. Lisbon, Portugal, pp. 101-106.
- Boltz, F., 2001, "Miniature Launch Vehicles for Very Small Payloads", *American Institute of Aeronautics and Astronautics, Journal of Spacecraft and Rockets*, Vol. 38, No. 1, pp. 126-128.
- Boltz, F., 2002, "Low-Cost Small-Satellite Delivery System", *American Institute of Aeronautics and Astronautics, Journal of Spacecraft and Rockets*, Vol. 39, No. 5, pp. 818-820.
- Braun, R. D. *et al.*, 1997, "Collaborative Approach to Launch Vehicle Design", *Journal of Spacecraft and Rockets*, Vol. 34, No. 4, 1997, pp. 478-486.

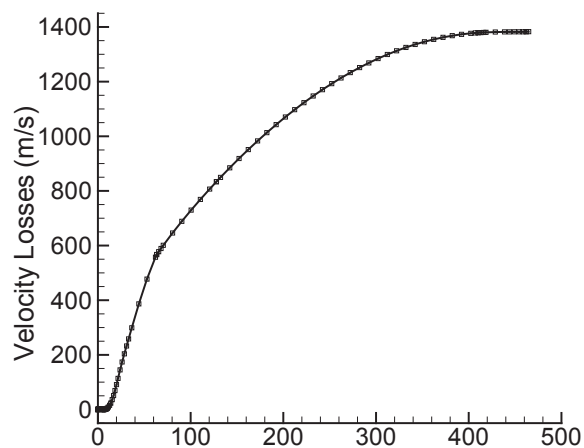


Figure 19. Accumulated velocity losses.

Blake, W. B., 1998, "Missile DATCOM user's manual".

Choi, Y. C. *et al.*, 2009, "Optimal air-launching rocket design using system trades and a multi-disciplinary optimization approach", *Aerospace Science and Technology*, doi:10.1016/J.ast.07.004, pp.1-9.

Fortescue, P. *et al.*, 2003, "Spacecraft Systems Engineering", 3rd Edition, Wiley.

Humble, R. W. *et al.*, 1995. "Space Propulsion Analysis and Design", 1st ed., M. A. Hollander, New York, McGraw-Hill.

Isakowitz, S.J. *et al.*, 2004, "International reference guide to space launch systems", 4th Ed., AIAA Inc.

Kafafy, R. *et al.*, 2011, "On The Scaling Laws for Air Launch Vehicles", *International Conference on Mechanical, Aerospace and Automotive Engineering ICMAAE'11*, Kuala Lumpur.

Lee, J.W. *et al.*, 2002, "Mission and trajectory Optimization of the Air-launching Rocket System Using MDO Techniques", *American Institute of Aeronautics and Astronautics, AIAA-2002-5492*, pp. 1-11, 9th AIAA/ISSMO Symposium on Multidisciplinary Analysis and Optimization Atlanta.

Lee, J.W. *et al.*, 2007, "Preliminary Design of the Hybrid Air-Launching Rocket for Nanosat", *Institute of Electrical and Electronics Engineers*, doi 10.1109/iccsa.2007.16, pp. 290-295.

Matsuda, S. *et al.*, 2008, "An Affordable Micro Satellite Launch Concept in Japan", *AIAA education series, RS6-2008-5004*, pp. 1-6.

Omar, H. *et al.*, 2011, "Particle Swarm Optimization of Air Launch Vehicle Trajectory". Canadian Aeronautics and Space Journal, Vol. 57, No. 2, pp. 115-120

Pegasus User's guide, 2007, approved for public release distribution Unlimited Release 6.0.

Sarigul-Klijn, N. *et al.*, 2005, "Air-launching Earth to Orbit: Effect of launch conditions and Vehicle Aerodynamics", Journal of Space and Rockets, Vol. 42, No. 3, pp. 569-572.

Storn, R., Price, K., 1995, "Differential evolution – a simple and efficient adaptive scheme for global optimization over continuous spaces", Technical Report TR-95-012.

Storn, R., Price, K., 1996, "Minimizing the real functions of the iccc'96 contest by differential evolution", Proceedings of IEEE International Conference on Evolutionary Computation, pp. 842-844.

Storn, R., 1996, "On the usage of differential evolution for function optimization", Fuzzy Information Processing Society, NAFIPS, 1996 Biennial Conference of the North American, pp. 519-523.

Storn R. *et al.*, Differential Evolution web site from <http://www.icsi.berkeley.edu/~storn/code.html>.

Storn, R. and Price, K., 1997, "Differential Evolution – A Simple and Efficient Heuristic for Global Optimization over Continuous Spaces", Journal of Global Optimization, No. 11, pp. 341-359.

Sutton, G. P. and Biblarz, O., 2010, "Rocket propulsion elements", 8th ed., New York, John Wiley & Sons.

Wong, K. P., Dong, Z. Y., 2005, "Differential Evolution, an Alternative Approach to Evolutionary Algorithm", IEEE, pp. 73-83.